Bial Foundation Grant Report (296/16) – Stephen Martin and Rosalina Fonseca

Synaptic competition and cooperation in reward learning: the role of hippocampal and prefrontal inputs to the nucleus accumbens

Final Report – 2021

Aims

The overall aim of this project was to study the synaptic mechanisms involved in the formation of associations between environmental information and reward that guide adaptive behaviour. Specifically, we investigated the properties of hippocampal and prefrontal inputs to the nucleus accumbens (NAc) using both cellular and systems-level approaches in rats. We now consider each of our specific aims in turn:

Aim 1: Identifying learning-related changes in synaptic strength in the hippocampal, PL, and IL inputs to the NAc

Introduction

Synaptic changes underlie memory formation in many brain areas, and the synapses that the hippocampal formation and prefrontal cortex make with neurons of the NAc provide a potential site for the formation, storage, and updating of associations between environmental stimuli, remembered information, action outcomes, and reward. The hippocampal formation is critical for the formation for memory for places and contexts, whereas the prefrontal cortex is involved in the processing of specific cues and their association with reward. Both of these structures send monosynaptic projections to the NAc (Boeijinga et al., 1993; Goto & Grace, 2005), and synaptic strength can be monitored in both pathways *in vivo*. To assess the potential role of these pathways in associative memory formation, we implanted rats with stimulating and recording electrodes to sample evoked synaptic responses and measure synaptic strength in these pathways while rats learned an association between a specific context and drug reward (administration of morphine) in a conditioned place preference (CPP) task.

Methods

After preliminary experiments to establish optimal coordinates, we implanted male Lister-hooded rats (n = 7) with chronic electrodes to record synaptic evoked field potentials (EFPs) in in the nucleus accumbens shell (NAcS) in response to electrical stimulation of the ventral hippocampus (vHPC). We also recorded local field potential (LFP) activity in the NAcS via the same electrode. The LFP is primarily a measure of spontaneous synaptic activity, and shows characteristic patterns of oscillatory activity, including theta (7-12 Hz) and gamma rhythms (~30-90 Hz). A separate group of rats (n = 3) was implanted with stimulating and recording electrodes to assess the time-course of morphine-induced EFP changes in the absence of CPP training.

Rats then underwent conditioned place preference (CPP) training in a 2-chambered apparatus in which one of two contexts with distinctive visual and tactile features was paired with morphine reward (10 mg/kg; SC), and the other with saline. Testing began with a single 45-min habituation session during which the rats were allowed to explore both chambers of the apparatus. This was followed by 8 days of conditioning in which each rat was confined to one chamber of the apparatus for 45 min immediately following saline injection, and the opposite chamber following morphine injection the next day. This was repeated for 8 days, with saline and morphine injections administered on alternating days. After the conditioning phase, rats received a 45-min probe trial in which they were allowed to explore both chambers; this was identical to the habituation trial. After a 1-week forgetting period, rats were tested during extinction for another 7 days; these sessions comprised a 45-min exploration of the whole apparatus (identical to the habituation and probe trials), and no injections were given. A drug-induced reinstatement trial was then conducted. This was identical to the extinction trials except that a 5 mg/kg priming dose of morphine was injected immediately before the trial.

Our original plan was to carry out similar recordings in projections from the medial prefrontal cortex to the NAcS. However, in preliminary experiments, we have been unable to record stable mPFC—NAcS evoked potentials in animals with chronically implanted electrodes. We are currently working to overcome these challenges.

Results

Administration of morphine led to a significant preference for the morphine-associated chamber in the initial probe trial, and priming administration of morphine caused a reinstatement of this preference after extinction (data not shown). Morphine administration caused an acute increase in the size of NAcS evoked responses, but no long-term changes were evident after conditioning or extinction of place preference (Fig. 1), suggesting that the formation of this type of memory does not lead to a net change in synaptic strength in the vHPC output to the NAc.

Fig. 2A shows an example of the mean power spectral density in the NAcS as a function of frequency, recorded during the habituation trial. There is a pronounced theta-frequency peak, and a modest gamma peak at around 60 Hz. After the final morphine injection, there was an increase in the amplitude, relative to the preceding saline day, of theta activity, and high-frequency gamma (60-90 Hz; Fig. 2B). Fig. 2C shows examples of LFP activity recorded during the final saline and morphine days of the conditioning phase, showing the increase in gamma activity in the latter. Despite the absence of learning-related changes in hippocampus – NAc evoked synaptic strength, the theta and gamma frequency LFP response to morphine became markedly sensitized with repeated administration, indicated by a progressive increase in the power of NAc theta (Fig. 3) and high-gamma-frequency activity (Fig. 4).

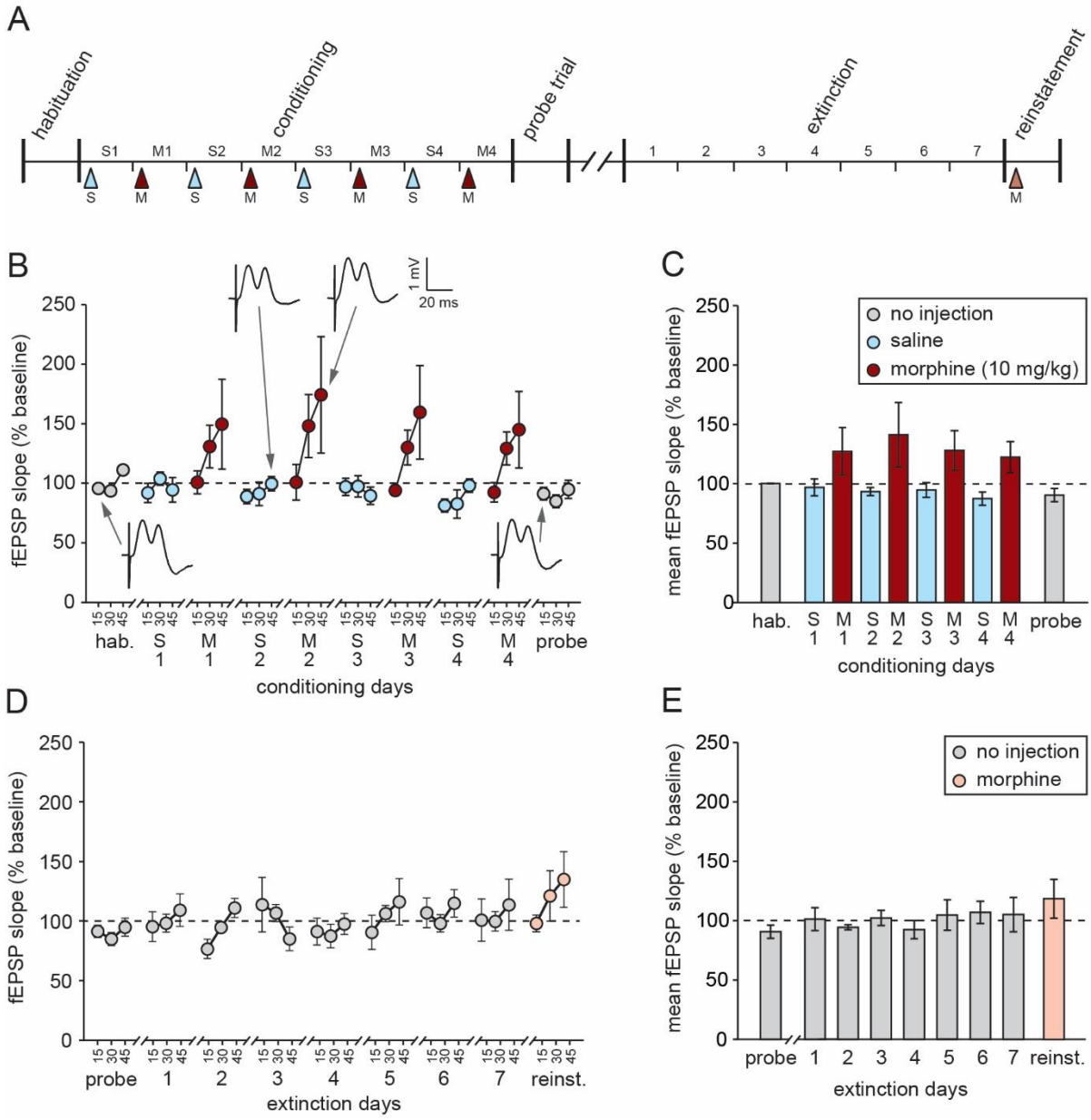

Figure 1. NAcS EFP slope data. (A) Timeline of experiment (S = saline injection; M = morphine injection; S1 = saline day 1; M1 = morphine day 1, etc.). (B) EFP slope during

habituation (hab.), conditioning, and probe trials, divided into 15-min time bins, and normalized to the mean value during habituation (100%) (S1 = saline day 1; M1 = morphine day 1, etc.). Representative examples are shown of EFPs recorded from the same rat during habituation, saline, morphine, and probe trials. A comparison of mean EFP slope values during habituation and probe trials—procedurally identical sessions—did not reveal a significant learning-related change [t(6)=1.73; p=0.14; paired-sample t-test]. During conditioning trials, little change was evident with and between saline days, but morphine caused a gradual rise in EFP slope throughout each session, although values always returned to baseline by the start of the subsequent saline session. An analysis of the mean EFP slope during the final 15 min of each conditioning session, revealed a significant increase on morphine relative to saline days [z=2.37; p=0.018; Wilcoxon signed-ranks test]. (C) Mean normalized EFP slope during the whole 45 min of each of the trials plotted in A. (D) EFP slope during probe, extinction, and reinstatement (reinst.) trials, divided into 15-min time bins, and normalized to the mean value during habituation (100 %). No overall changes in EFP slope were seen across the probe trial and successive extinction days [F(7,42)=0.782; p=0.606]. Injection of a priming dose of morphine revealed a small increase in the EFP slope, the mean EFP slope recorded during the final 15 min of the reinstatement trial was significantly higher than the mean of the corresponding time-point of the preceding 3 extinction days [z=2.03; p=0.043; Wilcoxon signed-ranks test]. (E) Mean normalized EFP slope during the whole 45 min of each of the trials plotted in D.

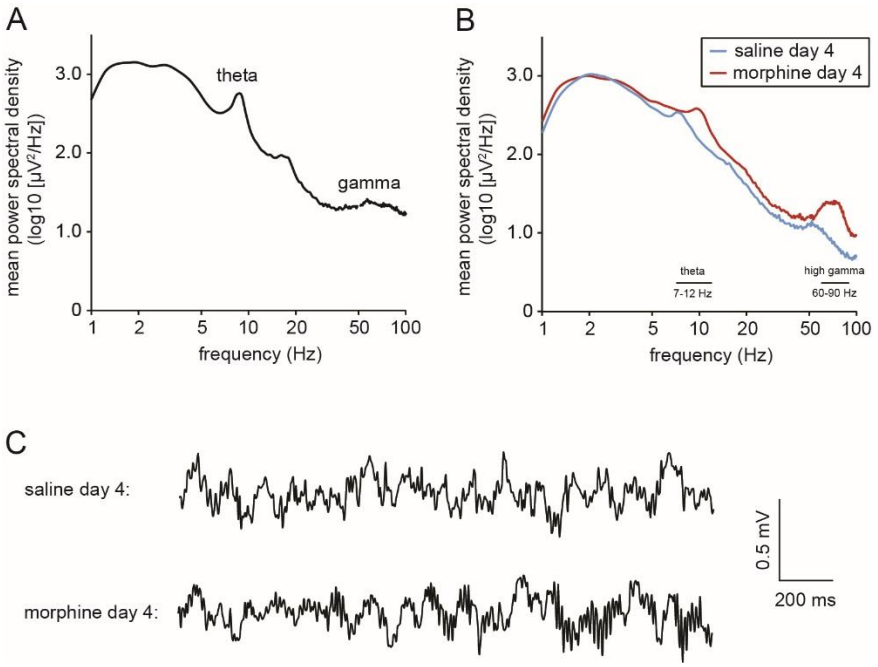

Figure 2. LFP power spectra. (A) Log-log plot of mean power spectral density as a function of frequency during the 45-min habituation trial for a single rat. (B) Mean power spectral density for the same rat during the final saline and morphine conditioning trials. Note the increase in theta and high gamma power in the latter. (C) Examples of 2-s periods of LFP activity recorded from the same rat during the final saline and morphine conditioning trials.

The acquisition of CPP did not result in any significant long-term change in theta-frequency activity in the absence of drug administration, indicated by the lack of a difference between habituation and probe trials [grey circles in Fig. 3A and grey bars in Fig. 3B; F(1,6) = 0.02; p = 0.89]. The same was true for high-gamma activity [Fig. 4A & B; F(1,6) = 4.44; p = 0.08]. However, during conditioning, a widening difference emerged between morphine and saline days in theta activity (Fig. 3A & B; red and blue circles/bars). An ANOVA in which drug (morphine versus saline), testing day (saline days 1-4 & morphine days 1-4), and time (i.e. within-session 15-min time-window) were all entered as within subjects factors revealed a significant overall difference in NAcS theta activity (7-12 Hz) between morphine and saline days [F(1,6) = 21.4; p = 0.004], and a significant drug x testing day interaction

[F(3,18) = 9.73; p < 0.0005]. A similar widening difference emerged between morphine and saline days in high-gamma activity (Fig. 4A & B; red and blue circles/bars). An ANOVA of mean NAcS high-gamma power (60-90 Hz) during conditioning days revealed a significant interaction of drug treatment and testing day [F(3,18) = 13.0; p < 0.002], with power increasing across successive morphine days [F(3,18) = 14.1; p = 0.0005] but remaining unchanged over successive saline days [F(3,18) = 0.48; p = 0.69].

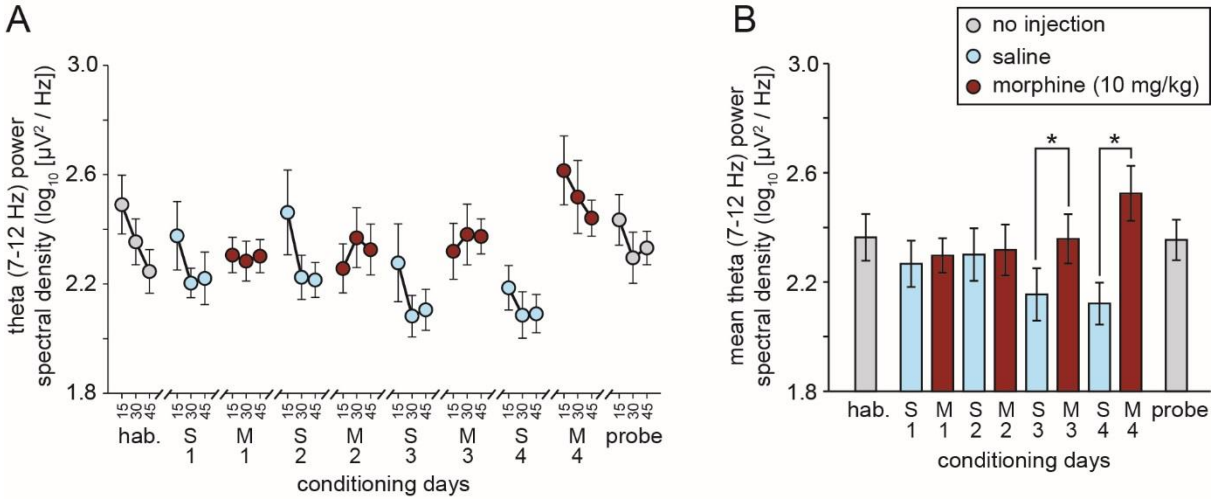

Figure 3. Morphine-induced sensitization of NAcS theta activity. (A) Theta power spectral density during habituation (hab.), conditioning, and probe trials, divided into 15-min time bins (S1 = saline day 1; M1 = morphine day 1, etc.). (B) Mean theta power spectral density during the whole 45 min of each of the trials plotted in A [*p < 0.05; paired-sample t-tests with Benjamini-Hochberg correction for multiple comparisons].

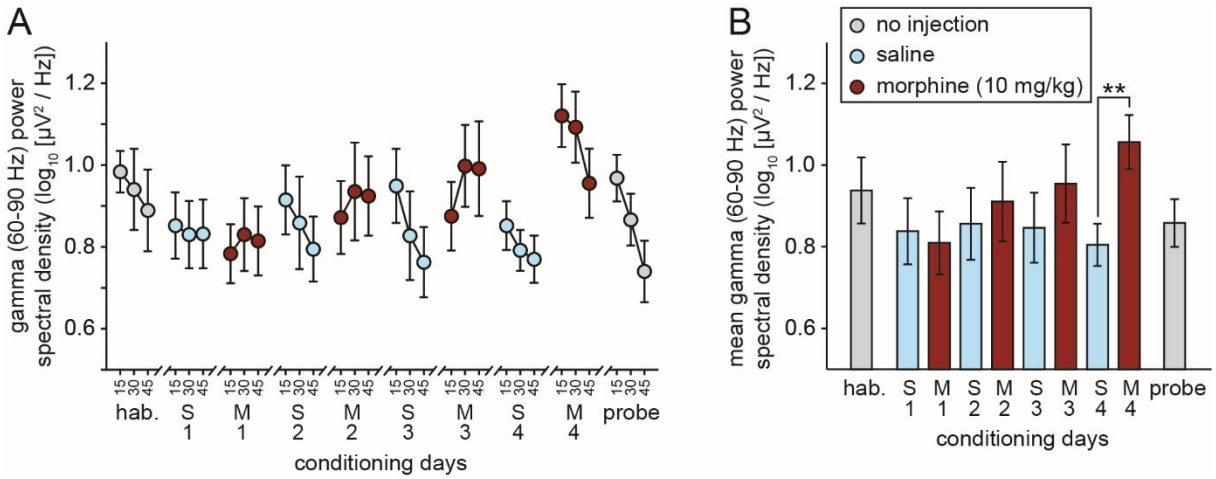

Figure 4. Morphine-induced sensitization of NAcS high-gamma activity. (A) Gamma power spectral density during habituation (hab.), conditioning, and probe trials, divided into 15-min time bins (S1 = saline day 1; M1 = morphine day 1, etc.). (B) Mean gamma power spectral density during the whole 45 min of each of the trials plotted in A [*p < 0.01; paired-sample t-test with Benjamini-Hochberg correction for multiple comparisons].

We also studied the time-course of morphine-induced evoked field potential (EFP) changes in a separate group of rats (n = 3) implanted with stimulating electrodes in the ventral hippocampus and recording electrodes in the NAc shell. (Fig. 5). This experiment revealed an acute increase in EFP amplitude and initial slope, an effect that reached a plateau within about 45 min of injection and was maintained for at least 6 h. However, the effect returned to baseline within 24 h. A statistical analysis was not conducted owing to the small number of animals, but all rats showed a morphine-induced increase in EFP slope.

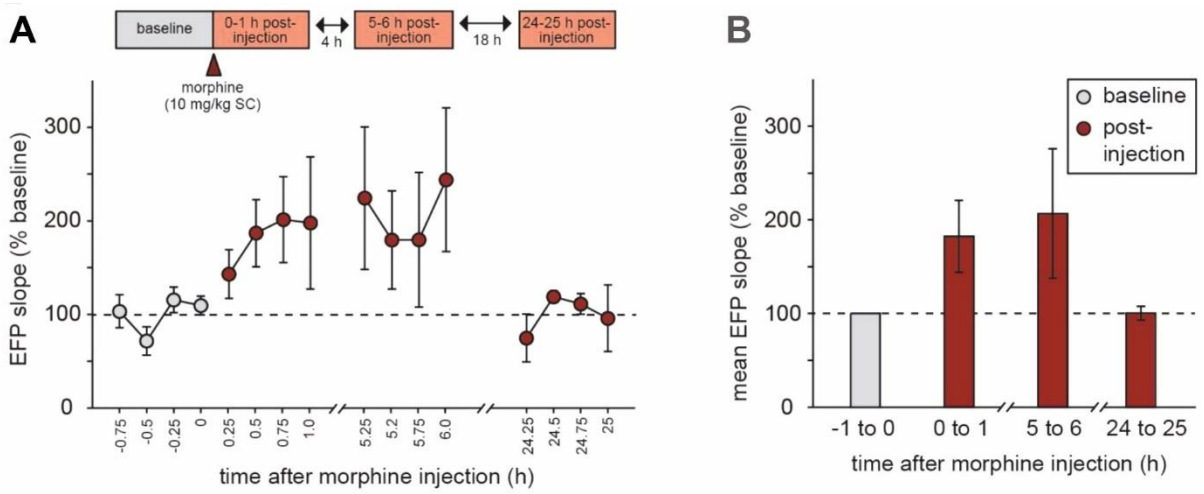

Figure 5. (A) Time course of the increase in EFP slope following morphine administration, normalized to the mean value over the 1-h period before injection (n = 3). (B) Summary of the data as shown in E, plotted as mean normalized hourly EFP slope values before and after morphine injection.

Aim 2: Properties of synaptic plasticity in the NAc *in vivo*

Introduction

The aim of this part of the programme was to characterise and study the properties of synaptic function and artificially induced synaptic plasticity in the prefrontal (infralimbic and prelimbic) and hippocampal projections to the nucleus accumbens, as well as the interactions between these inputs. While we were able to record evoked responses elicited by stimulation of prefrontal sites, and LTP could be induced in some cases by high-frequency electrical stimulation (see year 2 scientific report for more details), the amount of potentiation was highly variable, with little LTP in some cases. The same was true of electrically-induced LTP in the vHPC–NAcS projection. For this reason, we chose to focus primarily on the impact of opioid receptor activation on synaptic transmission in the vHPC–NAcS projection, comparing this with activity in the well characterised hippocampal projection from CA3 to CA1. This is highly relevant to the work presented in 'aim 1' in which opioid administration led to behavioural changes that paralleled the sensitisation of oscillatory activity in the NAcS.

Methods

The electrophysiological methods were similar to those used in 'aim 1', except that the rats were anaesthetised with urethane throughout the experiment. Male Lister-hooded rats were implanted with electrodes to record LFP activity in the NAcS. A separate group of rats was implanted with electrodes to record the LFP in the stratum radiatum (the dendritic layer) of area CA1 of the hippocampus. After the recording of a baseline, rats were injected with the mu opioid agonist buprenorphine (0.03 mg/kg, SC) or saline, and recording continued for a further 1 h. In a separate group of hippocampal recordings, a recording electrode was placed in the cell body layer of CA1 to record responses elicited by stimulation of Schaffer collaterals via a stimulating electrode placed in CA3. In this configuration, the evoked response comprises both a measure of synaptic strength—the slope of the early rising phase of the field excitatory postsynaptic potential (fEPSP slope)—and a measure of the stimulation-induced firing of action potentials—the population spike. Rats were again injected with buprenorphine (0.03 mg/kg, SC) and recording continued for a further 1 h.

Results

Injection of buprenorphine caused a broad spectrum increase in NAc LFP power in all animals tested, encompassing theta (3-6 Hz), beta (10-30 Hz) and gamma (50-70 Hz) frequency bands (Fig. 6A; n = 3). In contrast, buprenorphine caused a pronounced increase in beta and gamma activity in the dorsal hippocampus, but little change in theta (Fig. 6B; n = 3). No changes were observed in the dorsal hippocampus after saline injection (Fig. 6C; n = 3). A statistical analysis of these data is not presented owing to the small sample size, but these experiments are ongoing.

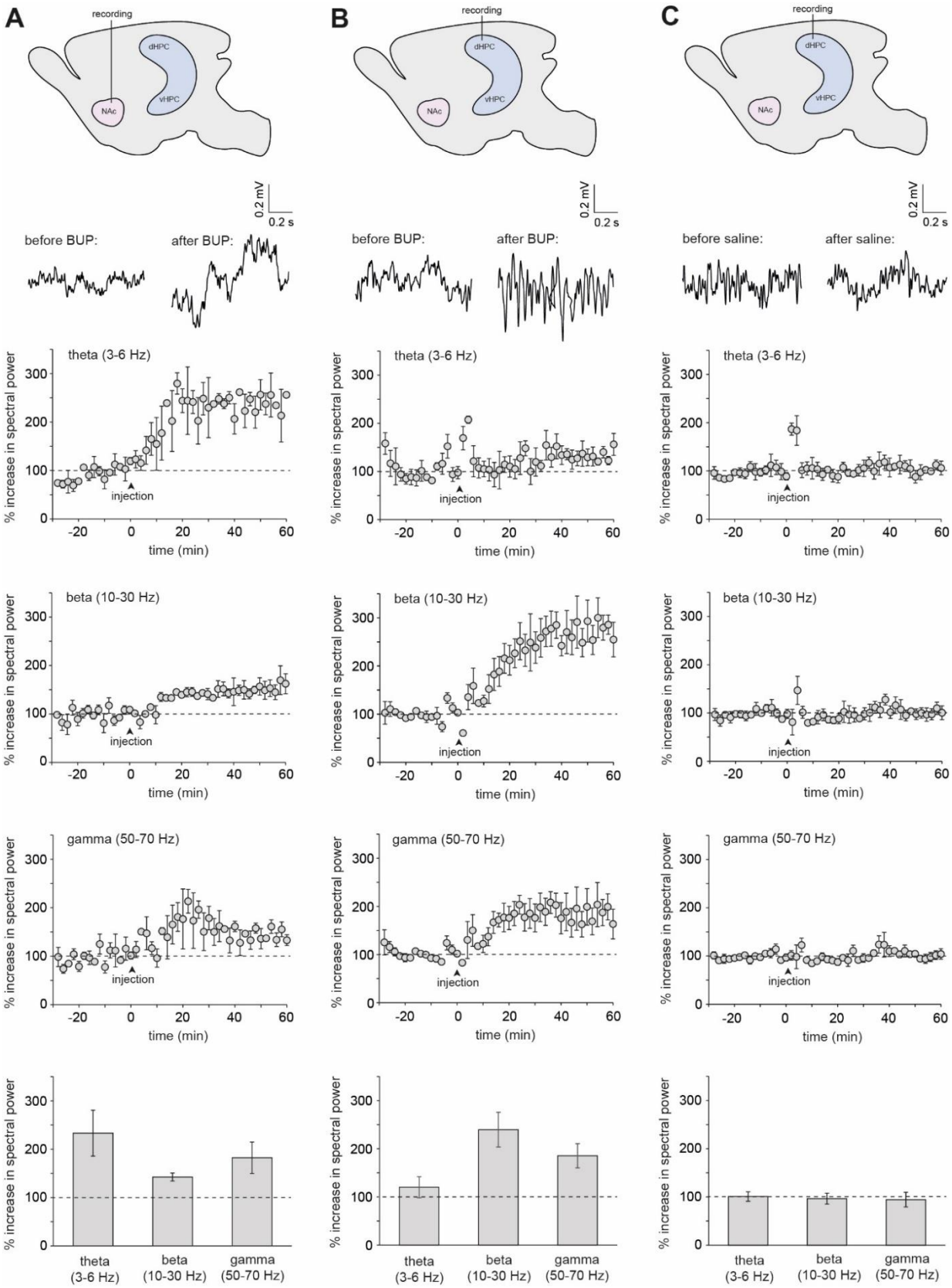

Figure 6. Upper panels show the location of the recording electrode in each condition, with 1-s samples of the LFP trace recorded before, and approximately 30 min after drug injection. The middle panels show the time course of the percentage change in LFP power, normalized to baseline values, within three frequency bands—theta (3-6 Hz), beta (10-30 Hz), and gamma (50-70 Hz). The lower panels show the mean percentage change in the three bands, 20-30 min after injection. (A) Buprenorphine caused an increase in power across all frequency bands in the NAc. (B) Buprenorphine caused an increase in beta and gamma, but not theta, power in dorsal CA1. (C) Saline (vehicle) injection had no effect on LFP activity in dorsal CA1.

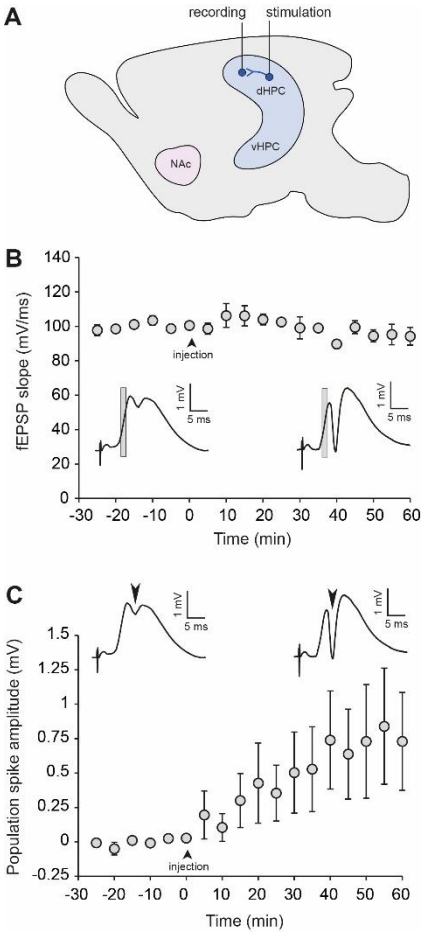

Recordings carried out in the cell body layer of area CA1 (Fig. 7A; n = 3) revealed that administration of buprenorphine had little impact on the fEPSP slope, a measure of AMPA-receptor-mediated fast synaptic transmission (Fig. 7B) but caused a large increase in the size of the population spike, a measure of the stimulation-induced firing of action potentials (Fig. 7C). A statistical analysis of these data is not presented owing to the small sample size, but these experiments are ongoing.

Figure 7. (A) Placement of stimulating and recording electrodes in the dorsal hippocampus to record extracellular evoked field potentials (fEPSPs). (B) Injection of buprenorphine had no effect on the fEPSP slope, indicating that the drug does not directly affect AMPA-receptor mediated fast synaptic transmission. Examples of fEPSPs recorded before and after drug administration are shown; the grey rectangles indicate the region of the fEPSP over which the slope measure was calculated. (C) Injection of buprenorphine caused a large increase in the amplitude of the population spike, indicated by the black arrowheads over the sample fEPSPs.

Aims 3&4: Properties of synaptic plasticity in the NAc *in vitro* and Competitive and cooperative interactions between prefrontal and hippocampal inputs to the NAc during the maintenance of LTP *in vitro*.

Introduction

Synaptic cooperation and competition are two forms of heterosynaptic plasticity that rely on the sharing of intracellular proteins among different sets of activated synapses (Pinho et al., 2020). Thus, inputs must terminate in the same neuron. We aim to test whether inputs from the hippocampus and the medial pre-frontal cortex (mPFC) to the nucleus accumbens (NAc) interact by cooperation leading to long-term changes in synaptic efficacy in both inputs. However, the NAc is anatomically and functionally divided in two subregions, the core and the shell, that differ in their functional connectivity to the hippocampus and the mPFC as well as in the expression of key modulators such as dopaminergic receptors (Scofield et al., 2016). Moreover, both the hippocampus and the mPFC can be divided in different subregions with different patterns of connectivity. The hippocampus can be further divided in the ventral and dorsal regions which show functional differences and also different patterns of connectivity with other cortical and subcortical areas (Fanselow and Dong, 2010). Similarly, the mPFC can be further divided in the prelimbic and infralimbic areas (Gorelova and Yang, 1996; Vertes, 2004). Given that we are focusing on the storage of associations between place or context and reward our test hypothesis was that the activation of the input from the prelimbic area of the mPFC and the input from the ventral hippocampus leads to the induction of an heterosynaptic cooperative increase in synaptic efficacy of both groups of synapses. As stated above, this means that prelimbic mPFC and ventral hippocampus synapses must terminate in the same groups of principal neurons within the NAc.

Considering the core and the shell subregions of the NAc, initial studies using electrophysiological approaches have shown a very high degree of convergence of hippocampus and mPFC inputs to both core and shell NAc subregions (French and Totterdell, 2002; O'Donnell and Grace, 1995). However, a recent study using virus-based labelling

technique to identify monosynaptic inputs to the core and shell subregions of the NAc has shown that the NAc core region is highly innervated by the prelimbic mPFC afferents whereas the hippocampus projection was more detectable in the shell NAc subregion (Li et al., 2018). Given this, we set out to analyse the distribution of hippocampal and mPFC input projections to NAc, using viral labelling.

Methods

All the experimental procedures were approved by the NOVA Medical School Animal Care and User Committee. For all experiments, we used Sprague-Dawley rats weighing 200g, housed at the animal facility in NOVA Medical School. All viruses were obtained from AddGene. For the double-labelling experiments we used two AAV virus, the AAV8-CaMKIIα-EGFP (*2,3x10^{13} infecting units per ml, Catalog #50469-AAV8, Addgene*) and the AAV8-hSyn-mCherry (*1,7x10^{13} infecting units per ml, Catalog #114472-AAV8, Addgene*). Before virus injection, animals were anesthetized using an isoflurane vaporizer (Kent Scientific) and mounted in a stereotaxic holder. After local anaesthesia with lidocaine (0.5%) a small craniotomy (0.5 mm diameter) was made above the targeted areas with a dental drill. For tracing, 600 nl of the AAV8-hSyn-mCherry was injected in the pre-limbic mPFC area (coordinates in mm AP: +3.24 DV: 3.40 ML: +/- 0.60; 1,38x10^{10} *infecting units per ml*) and 800nl of the AAV8-CaMKIIα-EGFP (1,36x10^{10} *infecting units per ml*) was injected in either the dorsal (dHip coordinates in mm AP: -3.84 DV: 2.40 ML: +/- 2.40) or the ventral hippocampus (vHip coordinates in mm AP: -5.52 DV: 5.80ML: +/- 5.80). Viruses were injected using a glass micropipette (30 µM tip size) connected to an injection system. The micropipette was held in place for 5 min after the injection before being slowly retracted from the brain. Two weeks later, animals were deeply anaesthetised using isoflurane and brains were collected for further histology processing. Brain tissue was collected and placed on a 4% PFA solution overnight for post-fixation. After dehydrated in 30% sucrose, brains were embedded in OCT and sectioned in 30µM sections using a cryostat. Imaging was performed using a confocal microscope in sections containing the NAc core and the shell.

Results

We used a double-labelling approach and focused in three brain areas, the prelimbic mPFC (PL mPFC) and the dorsal or ventral hippocampus regions. Each animal was either injected in the dorsal or the ventral hippocampus with the AAV8-CaMKIIα-EGFP (green) and the AAV8-hSyn-mCherry in the PL mPFC (red). Confocal images were then obtained in the shell and core NAc subregions. Regarding dorsal hippocampus and PL-mPFC, inputs from these areas were detected in both core and shell regions of the NAc although we found a predominance of mPFC inputs in the core region (Fig. 8A/B1 and B2).

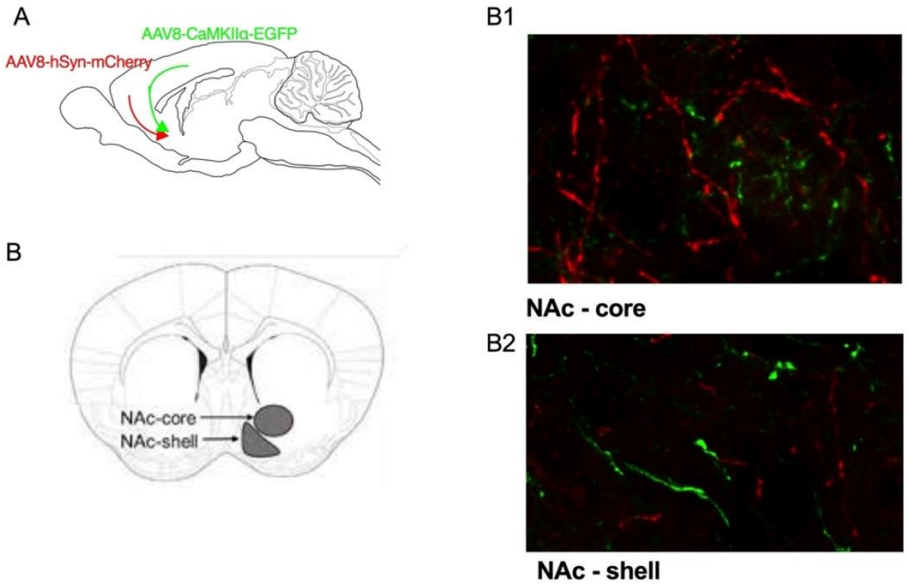

Figure 8. Injections were made in the pre-limbic mPFC and dorsal hippocampus (A). Images were taken in the NAc core and shell area (B). MIP of imaged areas within the core (B1) and shell (B2) NAc subregions. Red represent PL - mPFC projections, green represent dorsal hippocampus CA1 projections.

Interestingly, projections from the ventral hippocampus segregate between core and shell NAc regions. The ventral hippocampus is highly connected to the shell regions of the NAc, and we could not find any inputs from the ventral hippocampus in the core region of the NAc (Fig. 9A/B1 and B2). This observation was highly reproducible. From the three injected animals, all of then display the same patterns of connectivity.

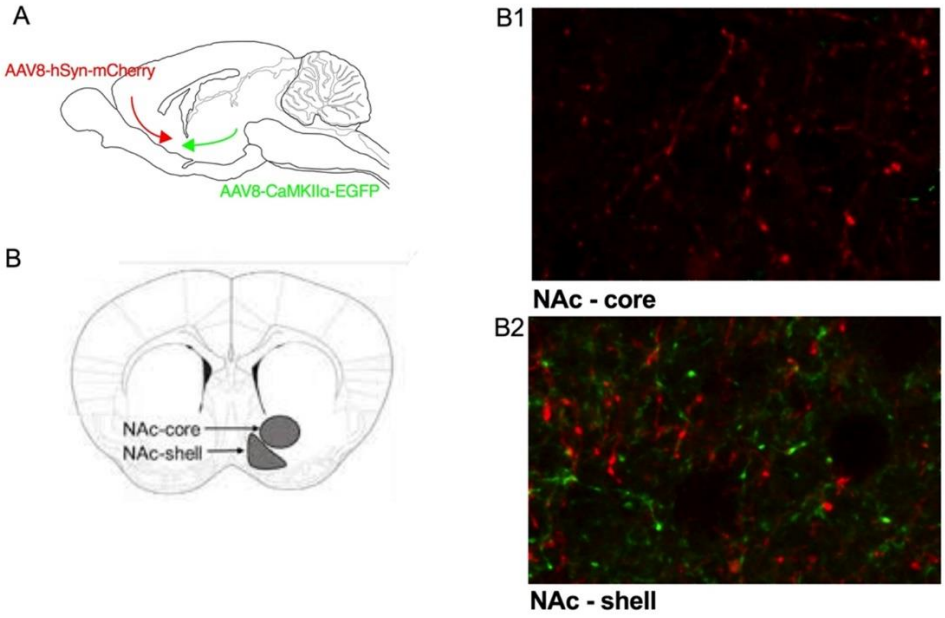

Figure 9. Injections were made in the pre-limbic mPFC and ventral hippocampus (A). Images were taken in the NAc core and shell area (B). MIP of imaged areas within the core (B1) and shell (B2) NAc subregions. Red represent PL - mPFC projections, green represent ventrla hippocampus CA1 projections.

General Discussion

Our first aim was to investigate the possibility that the learning of an association between context and reward causes learning-induced changes in synaptic strength. However, the formation of a morphine-conditioned place preference did not result in any changes in synaptic strength in the ventral hippocampal projection to the NAcS. This was indicated by the equivalent EFP slope values recorded during habituation to the testing apparatus, a post-conditioning probe trial, and during and after extinction of the context-morphine reward association. At face value, this result does not support the idea that VH-NAcS synapses are likely sites of storage for this form of memory. However, it is possible that learning-related changes occur sparsely or selectively in a small number of inputs, or that simultaneous increases and decreases in synaptic strength mask any overall change. It is also possible that the relevant learning-related changes occur upstream in the hippocampus itself, or in other structures altogether.

Despite the absence of learning-related changes in evoked potentials, there was a progressive increase in the power of NAc theta and high-gamma frequency activity with repeated morphine administration, an increase not observed after saline injection. NAc oscillations in the high-gamma frequency range are associated with reward expectancy in studies of natural reward (van der Meer et al., 2010), and the morphine-induced sensitisation of gamma activity that we have observed may provide an index of the incentive sensitisation process—the increased drug-seeking behaviour, drug craving, and association of environmental cues with drug reward—that accompanies repeated administration of opioids.

Morphine administration also caused an acute increase in the size of the accumbens EFP. An analysis of the time-course of the effect in a separate group of rats revealed a maximal increase at around 45 min after injection, and a complete return to baseline within 24 h. This effect was evident the first time that morphine was administered to each rat and remained constant with successive injections; the absence of sensitisation suggests an acute effect of the drug, rather than an association between context and drug reward. It is possible that this EFP increase reflects a reduction in feed-forward and feedback GABA-ergic inhibition, rather than direct postsynaptic enhancement of excitatory synaptic transmission at the medium spiny neurons—the principal neurons of the NAc. The activation of

mu-opioid receptors on GABA-ergic interneurons of the VTA, for example, disinhibits dopamine neurons, and a similar disinhibition of CA1 pyramidal cells has been reported in the dorsal hippocampus (see Nam et al., 2021 for review).

We have begun to investigate these phenomena in more detail as part of our ongoing research related to aim 2, comparing the impact of another mu opioid receptor agonist, buprenorphine, in the NAcS and area CA1 of the hippocampus. In anaesthetised rats, buprenorphine caused an increase in theta, and gamma activity, consistent with the actions of morphine in freely moving rats. However, unlike the effects of morphine, the effects of buprenorphine were evident after a single administration, a result that may reflect a greater potency of buprenorphine in inducing oscillatory activity. Similar effects were observed in dorsal CA1, except that changes in theta frequencies were minimal. To further investigate the ability of opioid receptor activation to disinhibit principal neurons, we studied the impact of buprenorphine on a well-characterised projection—the Schaffer collateral input to CA1. Drug administration caused a large increase in the amplitude of the population spike, a measure of the stimulation-evoked firing of CA1 neurons. This result is consistent with an increase in excitability caused by a reduction in GABA-ergic inhibition resulting from the activation of mu-opioid receptors located on GABA-ergic interneurons. As discussed above, the same phenomenon may underlie the increase in vHPC-NAcS EFPs observed in Fig. 1; we are planning to investigate the mechanisms of this phenomenon in more detail using *in vitro* techniques.

Our final objectives (3&4) were related to the interactions between prefrontal and hippocampal inputs to the NAc during LTP. However, our projection tracing data indicate that the degree of overlap between ventral hippocampal and the prelimbic mPFC inputs to the NAc is minimal and therefore, heterosynaptic cooperative associations between these two inputs cannot account for reward-induced context memory formation.

References

Boeijinga P, Mulder AB, Pennartz CMA, Manshanden I, & da Silva FHL (1993) Responses of the nucleus accumbens following fornix/fimbria stimulation in the rat. Identification and long-term potentiation of mono- and polysynaptic pathways. Neuroscience 53: 1049–1058.

Fanselow MS & Dong HW (2010). Are the dorsal and ventral hippocampus functionally distinct structures? Neuron 65: 7-19.

French S & Totterdell S (2002) Hippocampal and prefrontal cortical inputs monosynaptically converge with individual projection neurons of the nucleus accumbens. J Comp Neurol 446: 151-165.

Gorelova N & Yang CR (1996) The course of neural projection from the prefrontal cortex to the nucleus accumbens in the rat. Neuroscience 76: 689-706.

Gruber A, Hussain RJ, & O'Donnell P (2009) The nucleus accumbens: a switchboard for goal-directed behaviors. PloS One 4: e5062.

Goto Y & Grace AA (2005) Dopamine-dependent interactions between limbic and prefrontal cortical plasticity in the nucleus accumbens: disruption by cocaine sensitization. Neuron 47: 255–266.

Li Z, Chen Z, Fan G, Li A, Yuan J, & Xu T (2018) Cell-type-specific afferent innervation of the nucleus accumbens core and shell. Front Neuroanat 12: 84.

Magri C, Schridde U, Murayama Y, Panzeri S, & Logothetis NK (2012) The amplitude and timing of the BOLD signal reflects the relationship between local field potential power at different frequencies. J Neurosci 32: 1395-1407.

Martin SJ, Grimwood PD & Morris RGM (2000) Synaptic plasticity and memory: an evaluation of the hypothesis. Annu Rev Neurosci 23, 649–711.

Nam M-H, Won W, Han K-S, Lee CJ (2021) Signaling mechanisms of μ-opioid receptor (MOR) in the hippocampus: disinhibition versus astrocytic glutamate regulation. Cell Mol Life Sci 78: 415-426.

O'Donnell P & Grace AA (1995) Synaptic interactions among excitatory afferents to nucleus accumbens neurons: Hippocampal gating of prefrontal cortical input. J Neurosci 15: 3622-3639.

Pinho J, Marcut C, & Fonseca R (2020). Actin remodeling, the synaptic tag and the maintenance of synaptic plasticity. IUBMB Life 72: 577-589.

Sakae DY & Martin SJ (2019) formation of a morphine-conditioned place preference does not change the size of evoked potentials in the ventral hippocampus – nucleus accumbens projection. Sci Rep 9: 5206.

Scofield MD, Heinsbroek JA, Gipson CD, Kupchik YM, Spencer S, Smith ACW, Roberts-Wolfe D, & Kalivas PW (2016) The nucleus accumbens: mechanisms of addiction across drug classes reflect the importance of glutamate homeostasis. Pharmacol Rev 68: 816-871.

Van der Meer MAA, Kalenscher T, Lansink CS, Pennartz CMA, Berke JD, & Redish AD (2010) Integrating early results on ventral striatal gamma oscillations in the rat. Front Neurosci 4: 300.

Vertes RP (2004) Differential projections of the infralimbic and prelimbic cortex in the rat. Synapse 51: 32-58.